Unusual high-pressure intrusion-extrusion behavior of electrolyte solutions in Mu-26, a pure silica zeolite of topology STF

Carole Isaac, Giorgia Confalonieri, Habiba Nouali, Jean-Louis Paillaud, Rossella Arletti, T. Jean Daou, Andrey Ryzhikov

Unusual high-pressure intrusion-extrusion behavior of electrolyte solutions in Mu-26, a pure silica zeolite of topology STF

Carole Isaac[a,b], Giorgia Confalonieri[c], Habiba Nouali[a,b], Jean-Louis Paillaud[a,b], Rossella Arletti[c], T. Jean Daou[a,b,*], Andrey Ryzhikov[a,b,**]

[a] *Université de Haute Alsace, CNRS, Institut de Science des Matériaux de Mulhouse (IS2M), Axe Matériaux à Porosité Contrôlée (MPC), UMR7361, 68100, Mulhouse, France*
[b] *Université de Strasbourg, 67000, Strasbourg, France*
[c] *Dipartimento di Scienze Chimiche e Geologiche, Università Degli Studi Modena e Reggio Emilia, Via Campi 103, Modena, Italy*
** Corresponding author. 3 bis rue Alfred Werner, Mulhouse, F-68093, France.*
*** Corresponding author. 3 bis rue Alfred Werner, Mulhouse, F-68093, France.*
E-mail addresses: jean.daou@uha.fr (T.J. Daou), andrey.ryzhikov@uha.fr (A. Ryzhikov)

Received 4 November 2019; Received in revised form 7 January 2020; Accepted 23 January 2020 Available online 31 January 2020

To cite this article: Unusual high-pressure intrusion-extrusion behavior of electrolyte solutions in Mu-26, a pure silica zeolite of topology STF, Microporous Mesoporous Mater., 2020, 298, 110047. DOI : 10.1016/j.micromeso.2020.110047, HAL : hal-03065684.
Received 4 November 2019, Revised 7 January 2020, Accepted 23 January 2020, Available online 31 January 2020.

Abstract: High pressure intrusion-extrusion of LiCl aqueous solutions in Mu-26 zeolite (STF-type zeosil) has been studied. "Mu-26 – LiCl aqueous solution" systems have demonstrated an unusual combination of bumper and shock absorber behavior with several features and a high absorbed energy of 40.2 J/g. Contrary to other zeosils, the increase of LiCl concentration does not lead to an increase of intrusion reversibility. This phenomenon could be explained by the creation of higher amount of silanol defects inside the pores under LiCl aqueous solution infiltration. A highest rise of intrusion pressure (~6.6 times) with LiCl concentration among all the zeosils with similar pore diameter is observed. The pressure increase is accompanied with a strong rise of the intruded volume.

1. Introduction

High pressure intrusion-extrusion of nonwetting liquids in porous solids is one of the promising technologies of mechanical energy ab- sorption, dissipation, storage and generation [1–9]. Generally, "porous solid – non wetting liquid" systems, called also heterogeneous lyophobic systems (HLSs), are based on hydrophobic porous materials and water [10–15]. In 2001, the intrusion-extrusion of water in hydrophobic pure silica zeolites (zeosils) was studied for the first time by our team [16]. The systems based on hydrophobic zeolites are of high interest, due to their small pore opening, high intrusion pressure values (up to 180 MPa) and high stored energy density (up to 15 J/g) can be reached [17,18]. In order to improve the intrusion pressure and especially the stored energy, electrolyte aqueous solutions were used as nonwetting liquids for zeosils and other hydrophobic porous solids. They were found to be promising candidates to improve energetic performance of HLS by a considerable increase of intrusion pressure [19–24]. The first experiments performed on MFI-type zeosil showed, that the intrusion of highly concentrated LiCl aqueous solution gave rise of an intrusion pressure and, thus, of a stored energy up to three times in comparison with pure water - from 10 to 31 J/g [22]. Then, the study of intrusion of salt solutions was extended to other zeosils. It was found that this effect was particularly pronounced for the cage-type zeosils with small pore openings (CHA, DDR, LTA) [25–27]. The increase of intrusion pressure by 7.4 times was achieved for LTA-type zeosil using LiCl saturated solution (20 M) [27], whereas for channel-type zeosils, the pressure increased by a factor of 2–3 only [22,28–30]. This increase can be accounted for the energy required for the distortion of solvated ions and their partial desolvation under forced penetration into the micropores [27,31]. Nevertheless, osmotic phenomena remain also a possible explanation [24,32].

Depending on the nature of intruded liquid and porous solid struc- ture and composition, the HLS are able to restore, dissipate, or absorb irreversibly the suppled mechanical energy and therefore, displaying a spring, shock absorber, or bumper behavior, respectively. It is known that the behavior of zeosil-based systems depends on zeosil topology and the presence of silanol defects in the framework or their formation under intrusion. In the case of the intrusion of aqueous salt solutions, the HLS behavior can depend on the salt concentration. The intrusion of diluted aqueous salt solutions do not change significantly the behavior of the system, whereas the use of concentrated ones can change the behavior of some "zeosil — aqueous solution" systems. Generally, the intrusion of concentrated solutions leads to better reversibility [27,28,30,33] and improve the stability of the zeolite matrix [27,33].

The study of the intrusion-extrusion of electrolyte solutions in zeosils with different topologies is of high interest because it should allow to better understand the topology influence and the mechanism of salt solution intrusion. In this work, the intrusion-extrusion of LiCl aqueous solutions in Mu-26 zeolite (STF-type zeosil) has been studied. This zeosil possesses a framework with unidimentional 10 member-ring (10-MR) channels with side pockets. The zeosils with such structure have never been studied for the intrusion of aqueous salt solutions.

2. Experimental

Pure silica STF-type zeolite (Mu-26) was obtained in fluoride medium using 6,10-dimethyl-5-azoniaspiro[4,5]decane hydroxide

(DMASD) as a structure-directing agent and tetraethoxysilane (TEOS, Aldrich, 98%) as a silica source according to previous works [34,35]. The reaction gel with molar composition: 1 SiO_2: 0.25 DMASD: 0.25 HF (40%, Normapur): 5 H_2O was heated into a PTFE-lined stainless-steel autoclave at 150 °C for 30 days. The obtained powder was washed with deionized water, dried in an oven at 70 °C and calcined at 700°C during 5 h under oxygen flow. The obtained powder was very slightly gray, almost white, nevertheless the presence of a small quantity of unre- moved carbonaceous impurities is probable.

The intrusion-extrusion of water and LiCl aqueous solutions in Mu-26 samples was performed at room temperature using a Micromeritics mercury porosimeter (Model Autopore IV) with special cells with a piston containing preliminary outgassed zeosil powder (under vacuum at 300 °C) and corresponding solution. The measurements were performed with intrusion-extrusion cycle time of 1 h. The saturated LiCl solution was chosen because it is known to be highly effective in the improvement of HLS energetic performance due to a strong increase of intrusion pressure [22].

The samples after intrusion-extrusion experiments were washed with deionized water, dried in an oven at 70 °C and stored at room temper- ature and 80% RH. X-ray diffraction patterns of the different samples were recorded in a Debye Scherrer geometry on a STOE STADI-P diffractometer equipped with a curved germanium (111), primary monochromator, and a linear position-sensitive detector (6 ° 2θ) using Cu Kα, radiation (λ = 0.15406 nm). Measurements were achieved for 2θ angle values in the 4-90°range, step 0.04° 2θ, and time/step = 60 s. Nitrogen adsorption desorption isotherms were performed at -196 °C using a Micromeritics ASAP 2420 apparatus. Prior to the adsorption measurements, the samples were outgassed at 90 °C during 15 h under vacuum to eliminate physisorbed water, but to avoid the dehydroxylation process. The specific surface area (S_{BET}) and microporous volume (V_{micro}) were calculated using the BET and t-plot methods, respectively [36,37]. Thermogravimetric (TG) analyses were carried out on a Mettler Toledo STARe apparatus, under air flow, with a heating rate of 5 °C/min from 30 to 800 °C. The size and the morphology of the crystals were determined by scanning electron microscopy (SEM) using a Philips XL 30 FEG microscope. The ^{29}Si MAS and ^{1}H–^{29}Si CP-MAS NMR spectra were recorded at room temperature on a Bruker Advance II 300 MHz spectrometer, with a double-channel 7 mm Bruker MAS probe. The recording conditions are given in Table 1.

Table 1 Recording conditions of the ^{29}Si MAS and ^{1}H–^{29}Si CPMAS NMR Spectra.

	^{29}Si MAS	^{1}H–^{29}Si CP MAS
Chemical Shift Standard	TMSa	TMSa
Frequency (MHz)	59.6	59.6
Pulse width (μs)	2.60	5.00
Flip angle	π/6	π/2
Contact time (ms)	/	1
Recycle time (s)	80	5b
Spinning rate (kHz)	4	4
Scans number	1000	15000

[a] Tetramethylsilane.
[b] The relaxation time t1 was optimized.

3. Results and discussion

3.1. Intrusion-extrusion experiments

The intrusion-extrusion curves of "Mu-26 – H_2O and "Mu-26 – LiCl aqueous solution" systems are shown in Fig. 1. The intrusion-extrusion characteristics of the systems are summarized in Table 2. Three intrusion-extrusion cycles were performed, but only two of them are shown for each system except for "Mu-26 - 20 M LiCl aqueous solution" one, since the curves of the second and the following cycles are entirely overlapping. For the latter system, six intrusion-extrusion cycles were performed because of a haphazard variation of intrusion pressure observed between 2nd and 6th cycles (see below, Fig. S1 and Table 2). Only three cycles are presented in Fig. 1 in order to avoid the image overcharged. The water intrusion in the first cycle is partially irreversible, the extrusion occurs at a lower pressure than the intrusion, thus, the system demonstrates a combination of bumper and shock absorber behavior. In the following cycles, the intrusion becomes fully reversible and occurs over a wide pressure range, thus, the system demonstrates a spring behavior with very low hysteresis between intrusion and extrusion curves. These results are in agreement with the ones obtained in our previous work [35], only a slight increase of intruded volume (0.055 against 0.045 cm^3/g, respectively) and a slight decrease of intrusion pressure (49 against 51 MPa) have been observed. Partial irreversibility of intrusion in the first cycle and the decrease of intrusion pressure in the following ones are related to the formation of hydrophilic silanol defects in zeosil framework that is confirmed by the characterization of the samples after intrusion-extrusion tests (see below).

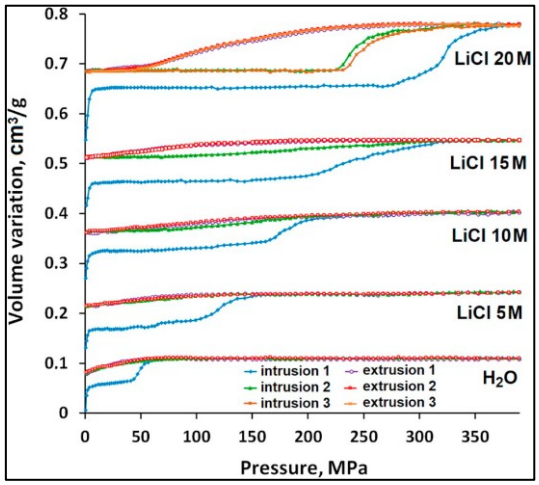

Fig. 1. Intrusion-extrusion curves of "Mu-26 – H_2O or LiCl aqueous solution"systems (5, 10, 15 and 20 M). The curves are shifted along the Y-axis for better visibility.

In the case of LiCl aqueous solutions intrusion-extrusion, the system behavior with a partially irreversible intrusion in the first cycle is quite similar. However, in the following cycles, the hysteresis between the intrusion and extrusion curves becomes more pronounced compared to "Mu-26 – water" system, that corresponds to a shock absorber behavior. The hysteresis increases with the rise of LiCl concentration and becomes very large for 15 and 20 M LiCl aqueous solution (energy yield of 35 and 48%, respectively). The phenomenon of slight increase of the hysteresis with LiCl concentration was previously observed for other "zeosil – solution" systems

[22], but in the case of Mu-26 the effect is particularly strong. Moreover, it should be noticed that such a large hysteresis is quite rare for "zeosil–LiCl aqueous solution" systems. A similar hysteresis for 20 M LiCl solution intrusion was only observed for DDR-type zeosil [26] and a slightly lower one for LTA-type zeosil [27], which have both a cage pore system. Such a shock absorber behavior has never been observed for the zeosils with channel pore system. Thus, it can be supposed that the presence of cages and side pockets in zeosil framework favors this behavior.

Table 2 Intrusion-extrusion characteristics of "Mu-26 – water or LiCl aqueous solution" systems.

	P_{int}[a] (MPa)	V_{int}[a] (cm^3/g)	P_{ext}[a] (MPa)	V_{ext}[a] (cm^3/g)	E_a[b] (J/g)	E_r[c] (J/g)	Yield[d] (%)	Behavior
Mu-26 - H_2O	49*/26**	0,055*/0,025**	24	0.025	2,7*/0.7**	0.6	22*/92**	B + SA*/S**
Mu-26 – LiCl 5 M	120*/66**	0.07*/0.02**	48	0.02	8.4*/1.3**	1	11*/72**	B + SA*/S**
Mu-26 – LiCl 10 M	180*/133**	0.08*/0.04**	109*/95**	0.04	14.4*/5.3**	4.2	30*/64**	B + SA*/S**
Mu-26 – LiCl 15 M	243*/203**	0.085*/0.035**	72**	0.035	20.6*/7.1**	2.5 12*/35**	12*/35**	B + SA*/S**
Mu-26 – LiCl 20 M	322*/223–249**	0.125*/0.08**	115	0.08	40.2*/19.2**	9.2	23*/48**	B + SA*/S**

*-first cycle, **-second and following cycles.
[a] Intrusion (P_{int}) and extrusion (P_{ext}) pressure, intruded (V_{int}) and extruded (V_{ext}) volumes determined from intrusion-extrusion isotherms for each step.
[b] Adsorbed energy E_a = Vint × Pint.
[c] Restored energy E_r = Vext × Pext.
[d] Energy yield = E_r/E_a × 100.

According to our previous studies on different zeosils, the use of concentrated LiCl aqueous solutions leads to an increase of intrusion reversibility in the first cycle of intrusion-extrusion [25,27,28,30]. For the systems with bumper behavior, the intrusion becomes more reversible with the rise of LiCl concentration. This can be explained by two different phenomena: 1). the solutions damage less the zeosil framework under intrusion, thus, a lower formation of hydrophilic silanol defects is observed; 2). the electrolyte solution interact less with silanol defects already present in the pores of zeolites, probably, due to a lower activity of water molecules which are totally included in solvation sphere of salt ions. However, in the case of Mu-26 zeolite, a different phenomenon is observed: the increase of LiCl concentration does not lead to the decrease of irreversibly intruded volume (V_{int} - V_{ext} for the 1st cycle). Moreover, this volume increases from 0.03 cm^3/g for water to 0.04–0.05 cm^3/g for all LiCl aqueous solutions. This effect could be explained by the formation of silanol groups even in the case of 20 M LiCl solution intrusion that was shown by the characterization of the samples before and after intrusion-extrusion experiments by solid-state

^{29}Si NMR and thermogravimetric analysis (see below). It seems that the structure of Mu-26 zeosil is particularly vulnerable to the damage by intruded liquid, since, according to our previous works, the intrusion of highly concentrated electrolyte solutions leads generally to lower silanol groups formation in comparison with water.

Another feature of the intrusion-extrusion of LiCl aqueous solutions in Mu-26 zeolite is a strong rise of total intruded volume with salt concentration. In the first cycle, the volume rises from 0.055 cm^3/g for water to 0.125 cm^3/g for 20 M LiCl aqueous solution, whereas for other zeosils, only a slight increase of intruded volume was previously observed (+10–20%) [22,25,27]. The only comparable impact was obtained in the case of DDR-type zeosil, where the intruded volume was also doubled [26].

It should be noticed that the values of intruded volume for LiCl solutions are higher than the one of micropore volume obtained from N_2 adsorption-desorption experiments (0.05 cm^3/g, see below). However, the latter is significantly lower than the one obtained in our previous work that can be related to the presence of a small number of silanol defects or carbonaceous species partially blocking unidimensional channels of the zeosil for N_2 molecules (see *Characterization* section). Under high pressure, water molecules and solvated ions penetrate into the pores interacting with silanol groups, whereas the carbonaceous species are removed by the liquid. Thus, the blocking effect disappears and the intruded species can entirely fill the channels. In the case of 20 M LiCl aqueous solution, the intruded volume is particularly high and close to a total filling of Mu-26 micropores [35], whereas the values of intruded volume in "zeosil–water or salt solution" systems are generally about 60% of the total micropore volume [38].

The rise of intrusion pressure with LiCl concentration is particularly strong. It increases by 6.6 times: from 49 MPa for pure water to 322 MPa for 20 M LiCl aqueous solution. It should be noticed that in most cases, the pressure rise is stronger for the zeosils with small pore openings. The highest values of this relative increase (5.6–7.4 times between water and 20 M LiCl aqueous solution) was previously observed only for the zeosils with 8 member-ring pore openings (CHA, DDR, LTA) [25–27], whereas the STF structure has 10-member ring pore openings. Generally, the zeosils with tridimensional 10-MRs channels (MFI, ITH-type zeosils) demonstrate an increase by 3.1–3.2 times in spite of similar pore diameter [22,30]. Such an effect can be related to the particularity of Mu-26 structure (STF topology) with unidimensional channels with side pockets. From the previous works [18,39], it is known that the water intrusion pressure is determined by a maximal pore diameter, which is relatively high in the case of Mu-26 because of large side pockets. Thus, the intrusion pressure of water is lower in comparison with other 10-MRs zeosils. In the same time, it was observed that the rise of intrusion pressure with LiCl solutions is determined by a size of pore openings [25–27]. The absolute value of intrusion pressure of 20 M LiCl aqueous solution in Mu-26 (322 MPa) is quite similar to ones for ITH- [30] and MFI-type [22] zeosils (280 and 283 MPa, respectively). Thus, it can be supposed that Mu-26 demonstrates a low intrusion pressure with water because of its side pockets and a high intrusion pressure with LiCl solutions due to its unidimensional channels that allows to explain such a strong increase of intrusion pressure with LiCl concentration.

Another interesting effect has been observed during the intrusion- extrusion of 20 M LiCl aqueous solution: the intrusion pressure in the second and following cycles is not the same, but varies randomly from one cycle to another in the range of 223–249 MPa (242, 249, 225, 229, 223 for 2nd, 3rd, 4th, 5th and 6th cycle, respectively). This phenomenon has never been observed before and remains unexplained for us. It may be supposed that it is related to a rearrangement of non-extruded species within the pores.

It should be also noticed that the system "Mu-26 - 20 M LiCl aqueous solution" demonstrates very high value of absorbed energy (40.2 J/g), particularly due to high intrusion pressure value (P_{int} = 322 MPa). This is the second highest energy obtained for zeosil-based systems after the "DDR-type zeosil – 20 M LiCl aqueous solution" one, where the absorbed energy of 93 J/g was attaint [26].

3.2. Characterization

The powder X-ray diffraction (PXRD) patterns of Mu-26 samples before and after three intrusion-extrusion cycles are shown in Fig. 2. The presence of a small quantity of amorphous phase is observed for the calcined parent material as well as for the post treated ones. The high- pressure post-treatments lead to an interesting modification of the symmetry. In Table 3, the indexation of the PXRD patterns determined from the Louer algorithm [40] and after Le Bail refinements (Fig. S2) [41] clearly shows the evolution from a triclinic to a monoclinic lattice when calcined Mu-26 is intruded with water. This transformation is unexpected but interesting. Indeed, as-made Mu-26 is triclinic (non-- centrosymmetric space group *P*1) [34] as the corresponding calcined product (centrosymmetric space group *P*-1) [42]. The intrusion of water seems to modify the lattice into the monoclinic one that corresponds exactly to the highest maximal STF topology with a double unit cell volume as it was observed experimentally in e.g. as-made (S.G. *C*2/*m*) [F,DMABO]-STF [43] and calcined ITQ-9 after a triclinic lowering of the symmetry (S.G. *I*-1) [44].

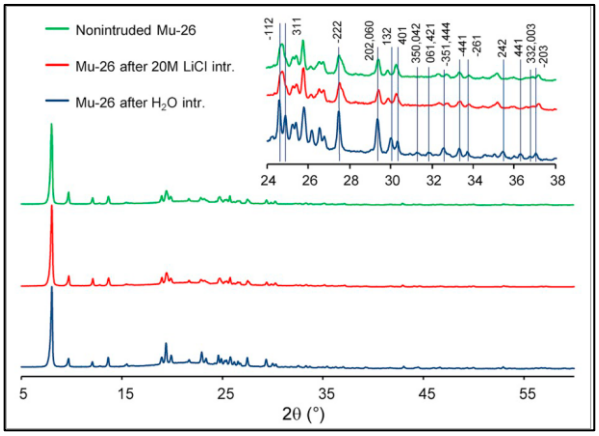

Fig. 2. Powder X-ray diffraction patterns of calcined Mu-26 (STF-type zeosil) samples before and after intrusion-extrusion experiments with water and 20 M LiCl aqueous solution. The insert is a magnification of the patterns that highlights the differences between the triclinic lattices before and after intrusion of a 20 M LiCl solution and the monoclinic lattice after water intrusion on calcined Mu-26. The vertical bars with Miller indices are guides corresponding to the monoclinic lattice.

Contrary to water, no structural evolution is observed when 20 M LiCl solution is intruded. It could be supposed that this is related to a different nature of extraframework species under high pressure intru- sion. In the case of water, the filling of the pores by water molecules and the formation of silanol groups is possibly favorable for the phase transformation, whereas in the case of LiCl solution, the quantity (V_{int}) and the arrangement of intruded ions are different and they can interact differently with silanol defects blocking the lattice transformation.

The crystal morphology of the STF-type zeosil was examined by scanning electron microscopy. No difference between nonintruded and intruded samples was found. SEM image is presented in Fig. 3, where large faceted crystals of irregular shape with a size ranging from 20 to 100 μm are observed.

Table 3 Unit cell parameters of calcined Mu-26 before and after intrusion–extrusion of water or 20 M LiCl aqueous solution after Le Bail refinement with GSAS-II software [45].

	Calcined Mu-26	Mu-26 - H_2O	Mu-26 - LiCl 20 M
Space Group	*P*-1	*C*2/*m*	*P*-1
a (Å)	11.438(2)	13.944(1)	11.443(3)
b (Å)	11.517(2)	18.225(1)	11.514(3)
c (Å)	7.3939(5)	7.4164(4)	7.393(1)
α (°)	94.846(3)	90	94.855(4)
β (°)	95.962(4)	99.031(3)	95.951(5)
γ (°)	104.924(7)	90	104.927(8)
V (Å^3)	929.73(8)	1861.42(10)	929.8(3)
GOF[a]	1.87	1.87	1.72

[b] Goodness of fit [45].
[a] C-centering mode.

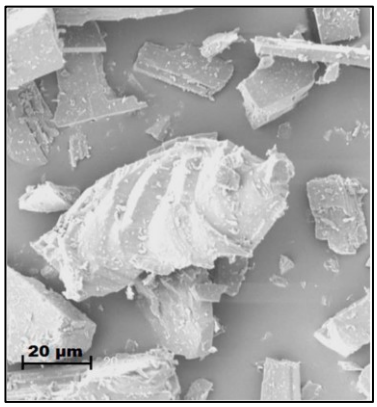

Fig. 3. SEM micrograph of nonintruded Mu-26 (STF-type zeosil) sample.

The N_2 adsorption desorption isotherms of Mu-26 zeolite before and after three intrusion-extrusion cycles are depicted in Fig. 4. The isotherms are mainly of type I characteristic of microporous solids. The values of BET surface area and micropore volume of calcined Mu-26 sample before intrusion are quite low 128 m^2/g and 0.05 cm^3/g, respectively, this is considerably lower than that obtained in our pre- vious work on STF-type zeosil (296 m^2/g and 0.11 cm^3/g) [35]. It can be assumed that part of the porosity is not accessible for nitrogen molecules because of the presence of silanol defects or unremoved carbonaceous species which can block the unidimensional channels in spite of their small number. The TG results (Fig. 5) confirm that nonintruded Mu-26 sample contains more silanol groups than the one studied previously [35]. Similar to the previous work, a strong decrease of micropore vol- ume and BET surface area is observed for the samples after intrusion-extrusion tests, up to 32 m^2/g and 0.01 cm^3/g for the one after 20 M LiCl solution intrusion and up to 4 m^2/g and close to ~0 cm^3/g for water-intruded one. This drop can be explained by a higher number of silanol defects and strongly adsorbed molecules of water or electrolyte blocking the access in the pores as it is confirmed by the TG results (Fig. 5).

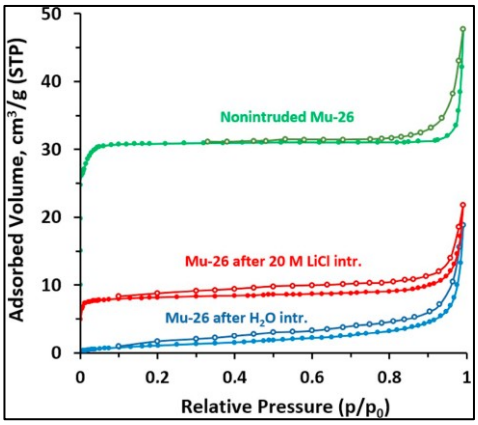

Fig. 4. N_2 adsorption desorption isotherms at 196 °C of Mu-26 (STF-type zeosil) samples before and after intrusion-extrusion experiments with water and 20 M LiCl aqueous solution. Filled and hollow symbols correspond to adsorp- tion and desorption isotherms, respectively.

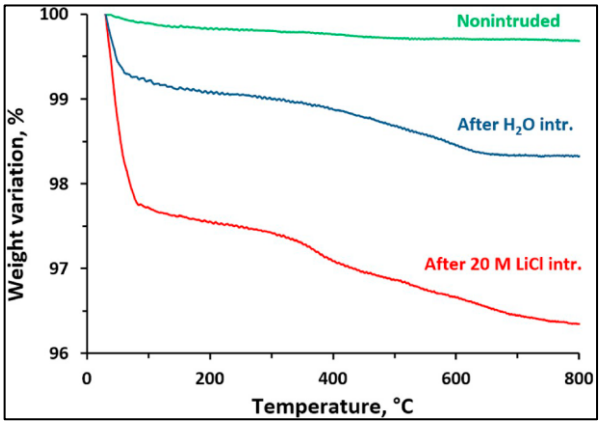

Fig. 5. Thermogravimetric curves of Mu-26 (STF-type zeosil) samples before and after intrusion-extrusion experiments with water and 20 M LiCl aqueous solution.

As it was mentioned above, the silanol defects are formed under intrusion-extrusion experiments as it follows from the results of thermal analysis (Fig. 5) and Si NMR spectroscopy (Fig. 6). According to TGA, the nonintruded Mu-26 sample demonstrates a highly hydrophobic character (total weight loss of 0.5 wt%). Nevertheless, it contains more silanol defects in comparison with the one from our previous work [35], 0.1 group per unit cell against 0.03. This can explain a slightly lower value of intrusion pressure and a lower value of pore volume obtained by N_2 adsorption-desorption because of stronger occulting of the volume of unidimensional channels by the silanols. After intrusion-extrusion ex- periments, the total weight loss increases considerably up to 1.7 and 3.6 wt% for water and 20 M LiCl solution, respectively. The weight loss step at low temperature (< 100 °C) is ascribed to the desorption of phys- isorbed water molecules and followed by the desorption of strongly physisorbed ones (100-350 °C). The sample after 20 M LiCl intrusion contains more physisorbed water. The weight loss in the temperature range of 350-800 °C is attributed to dehydroxylation reactions of silanol groups arising from the breaking of siloxane bridges under intrusion. It has been observed that the intrusion-extrusion experiments lead to a considerable increase of silanol content in Mu-26 framework. This weight loss step corresponds to 0.7 and 1.1 OH groups per unit cell (the chemical composition of a defect free STF-type zeosil being $[Si_{16}O_{32}]$) of Mu-26 for water and 20 M LiCl intruded samples, respectively.

The results of thermogravimetric analysis are confirmed by ^{29}Si MAS NMR spectroscopy (Fig. 6). The spectrum of the nonintruded sample has six main resonances in the range of 105 to 114 ppm corresponding to the non-equivalent crystallographic silicon Q_4 ($Si(OSi)_4$) sites. After intrusion-extrusion experiments, these resonances overlap more and new resonances of lower intensities attributed to Q_3 ($(SiO)_3Si-OH$) sites appear in the 92 to 97 ppm range. The ratio Q_3/Q_4 signals corre- sponds to approximately 1.1 and 1.2 silanol defect per unit cell for the samples intruded with water and 20 M LiCl solution, respectively. The ^{1}H–^{29}Si CPMAS NMR spectra of Mu-26 zeosil (insert in Fig. 5) confirm the increase of Q_3 sites content in the intruded samples. Thus, it can be concluded that the formation of silanol defects is similar or, according to the TG results, even higher in the case of the intrusion-extrusion of 20 M LiCl aqueous solution than in the one of water. This is a feature of Mu-26 zeolite, since an opposite trend was observed for all other zeosils studied previously, where an intrusion of highly concentrated LiCl solutions leaded to lower formation of defects. Thus, the formed silanol groups are probably responsible for the partially irreversible intrusion in Mu-26 sample in the 1st cycle. A part of intruded water molecules and sol- vated ions interact with the defects and remain trapped inside the pores.

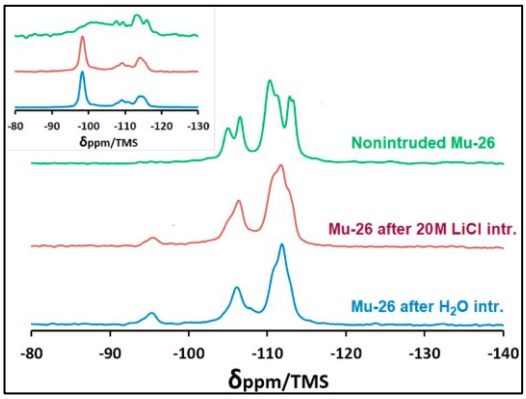

Fig. 6 ^{29}Si MAS NMR spectra of Mu-26 samples before and after intrusion- extrusion experiments with water and 20 M LiCl aqueous solution. The insert shows the corresponding ^{1}H–^{29}Si CPMAS NMR spectra.

4. Conclusions

In this work, a high pressure intrusion-extrusion of LiCl aqueous solutions in Mu-26 zeolite (STF-type zeosil) having a framework with unidimensional 10 member-ring channels with side pockets, has been performed. It has been shown that among other zeosil-based systems, the "Mu-26 – LiCl aqueous solution" ones exhibit an unusual behavior probably related to the particularities of the framework. The features of high pressure intrusion-extrusion of LiCl aqueous solutions in Mu-26 zeolite are the following:

- For concentrated LiCl aqueous solutions, Mu-26-based systems show a combination of bumper and shock-absorber behavior in the first cycle and a shock-absorber behavior with a large hysteresis between intrusion and extrusion curves in the following ones. The hysteresis increases with the concentration of LiCl aqueous solution, that is quite unusual for the most part of zeosil-based HLS.
- Similar to water, the intrusion of the LiCl aqueous solutions is partially irreversible. However, the volume of nonextruded liquid increases compared to the "Mu-26 – water" system, whereas for all other zeosils studied, the rise of LiCl concentration leads to an improvement of intrusion reversibility. This phenomenon can be explained by a formation of silanol defects under intrusion of LiCl solutions.
- "Mu-26 – LiCl aqueous solution" systems demonstrate a strong rise (by 6.6 times in comparison with water) of intrusion pressure with LiCl concentration. Such an increase was previously obtained only for the zeosils with small 8 MRs pore openings (5.6 – 7.4 times), whereas Mu-26 has larger 10 MRs ones.
- A strong rise of intruded volume with LiCl concentration is observed. The volume rises from 0.055 cm^3/g for water to 0.125 cm^3/g for 20 M LiCl solution, whereas only slight increase of intruded volume with salt concentration is observed for the most part of "zeosil – solution" systems.
- "Mu-26 – 20 M LiCl aqueous solution" system demonstrates the second highest value of absorbed energy obtained for zeosil-based systems (40.2 J/g).
- During the intrusion-extrusion of 20 M LiCl aqueous solution, the intrusion pressure in the second and following cycles is not the

same, but it varies randomly from one cycle to another in the range 223 – 249 MPa. This phenomenon has never been

Declaration of competing interest

The authors declare that they have no known competing financial interests or personal relationships that could have appeared to influence the work reported in this paper.

CRediT authorship contribution statement

Carole Isaac: Investigation. **Giorgia Confalonieri:** Investigation. **Habiba Nouali:** Investigation. **Jean-Louis Paillaud:** Methodology. **Rossella Arletti:** Writing - review & editing. **T. Jean Daou:** Concep- tualization, Supervision, Writing - original draft, Writing - review & editing. **Andrey Ryzhikov:** Conceptualization, Supervision, Writing - original draft, Writing - review & editing.

Appendix A. Supplementary data

Supplementary data to this article can be found online at https://doi. org/10.1016/j.micromeso.2020.110047.

References

[1] V.A. Eroshenko, Heterogeneous structure for accumulation or dissipation of energy, process to use it and associated devices. Int. Patent WO96/18040 (1996).

[2] V.A. Eroshenko, Interfacial energy in the lyophobic systems and challenge to all physico-chemists. In The Eights International Conference on Material Technologies and Modeling, MMT-2014, Ariel, Israel.

[3] V.A. Eroshenko, A. Popyk, Int. J. Therm. 17 (2014) 33–41, https://doi.org/ 10.5541/ijot.509.

[4] L. Coiffard, V.A. Eroshenko, J.P.E. Grolier, AIChE J. 51 (2005) 1246–1257, https:// doi.org/10.1002/aic.10371.

[5] A. Laouir, L. Luo, D. Tondeur, T. Cachot, P. Le Goff, AIChE J. 49 (2003) 764–781, https://doi.org/10.1002/aic.690490320.

[6] V.A. Eroshenko, I. Piatiletov, L. Coiffard, V.P. Stoudenets, Proc. Inst. Mech. Eng. - Part D J. Automob. Eng. 221 (2007) 301–312, https://doi.org/10.1243/ 09544070D01605.

[7] V.A. Eroshenko, Proc. Inst. Mech. Eng. - Part D J. Automob. Eng. 221 (2007) 285–300, https://doi.org/10.1243/09544070d01505.

[8] C.V. Suciu, T. Iwatsubo, K. Yaguchi, M. Ikenaga, J. Colloid Interface Sci. 283 (2005) 196–214, https://doi.org/10.1016/j.jcis.2004.08.034.

[9] C.V. Suciu, K. Yaguchi, Exp. Mech. 49 (2009) 383–393, https://doi.org/10.1007/ s11340-008-9163-z.

[10] A.Y. Fadeev, V.A. Eroshenko, J. Colloid Interface Sci. 187 (1997) 275–282, https:// doi.org/10.1006/jcis.1996.4495.

[11] T. Martin, B. Lefevre, D. Brunel, A. Galarneau, F. Di Renzo, F. Fajula, P.F. Gobin, J. Quinson, G. Vigier, Chem. Commun. (J. Chem. Soc. Sect. D) 1 (2002) 24–25, https://doi.org/10.1039/B109081J.

[12] B. Lefevre, A. Saugey, J.-L. Barrat, L. Bocquet, E. Charlaix, P.F. Gobin, G. Vigier, Colloids Surf., A 241 (2004) 265–272, https://doi.org/10.1016/j. colsurfa.2004.04.020.

[13] G. Ortiz, H. Nouali, C. Marichal, G. Chaplais, J. Patarin, Phys. Chem. Chem. Phys. 15 (2013) 4888–4891, https://doi.org/10.1039/c3cp00142c.

[14] Y. Grosu, M. Li, Y.-L. Peng, D. Luo, D. Li, A. Faik, J.-M. Nedelec, J.-P. Grolier, ChemPhysChem 17 (2016) 3359–3364, https://doi.org/10.1002/cphc.201600567.

[15] G. Ortiz, H. Nouali, C. Marichal, G. Chaplais, J. Patarin, J. Phys. Chem. C 118 (2014) 21316–21322, https://doi.org/10.1021/jp505484x.

[16] V. Eroshenko, R. Regis, M. Soulard, J. Patarin, J. Am. Chem. Soc. 123 (2001) 8129–8130, https://doi.org/10.1007/s11340-008-9163-z.

[17] L. Tzanis, M. Trzpit, M. Soulard, J. Patarin, Microporous Mesoporous Mater. 146 (2011) 119–126, https://doi.org/10.1016/j.micromeso.2011.03.043.

[18] L. Tzanis, M. Trzpit, M. Soulard, J. Patarin, J. Phys. Chem. C 116 (2012) 20389–20395, https://doi.org/10.1021/jp305632m.

[19] F.B. Surani, Y. Qiao, J. Appl. Phys. 100 (2006), https://doi.org/10.1063/ 1.2222042, 034311-5.

[20] X. Kong, Y. Qiao, Appl. Phys. Lett. 86 (2005), https://doi.org/10.1063/1.1901830, 151919.

[21] M. Soulard, J. Patarin, Process for High-Pressure Energy Storage by Solvation/ Desolvation and Associated Storage Device, 2011. Patent FR2976030.

[22] L. Tzanis, H. Nouali, T.J. Daou, M. Soulard, J. Patarin, Mater. Lett. 115 (2014) 229–232, https://doi.org/10.1016/j.matlet.2013.10.063.

[23] G. Fraux, F.X. Coudert, A. Boutin, A. Fuchs, Chem. Soc. Rev. 46 (2017) 7421–7437, https://doi.org/10.1039/C7CS00478H.

[24] M. Michelin-Jamois, C. Picard, G. Vigier, E. Charlaix, Phys. Rev. Lett. 115 (2015), https://doi.org/10.1103/PhysRevLett.115.036101, 036101.

[25] L. Ronchi, A. Ryzhikov, H. Nouali, T.J. Daou, J. Patarin, New J. Chem. 47 (2017) 2586–2592, https://doi.org/10.1039/C6NJ03730E.

[26] L. Ronchi, A. Ryzhikov, H. Nouali, T.J. Daou, J. Patarin, J. Phys. Chem. C 122 (2018) 2726–2733, https://doi.org/10.1021/acs.jpcc.7b10995.

[27] A. Ryzhikov, L. Ronchi, H. Nouali, T.J. Daou, J.-L. Paillaud, J. Patarin, J. Phys. Chem. C 119 (2015) 28319–28325, https://doi.org/10.1021/acs.jpcc.5b09861.

[28] L. Ronchi, A. Ryzhikov, H. Nouali, T.J. Daou, S. Albrecht, J. Patarin, Microporous Mesoporous Mater. 254 (2017) 153–159, https://doi.org/10.1016/j. micromeso.2017.02.064.

[29] L. Ronchi, A. Ryzhikov, H. Nouali, T.J. Daou, J. Patarin, Microporous Mesoporous Mater. 255 (2018) 211–219, https://doi.org/10.1016/j.micromeso.2017.07.039.

[30] L. Ronchi, A. Ryzhikov, H. Nouali, T.J. Daou, J. Patarin, New J. Chem. 41 (2017) 15087–15093, https://doi.org/10.1039/C7NJ03470A.

[31] G. Confalonieri, A. Ryzhikov, R. Arletti, H. Nouali, S. Quartieri, T.J. Daou, J. Patarin, J. Phys. Chem. C 122 (2018) 28001–28012, https://doi.org/10.1021/ acs.jpcc.8b07338.

[32] T. Humplik, J. Lee, S. O'Hern, T. Laoui, R. Karnik, E.N. Wang, Nanotechnology 28 (2017), https://doi.org/10.1088/1361-6528/aa9773, 505703.

[33] A. Ryzhikov, I. Khay, H. Nouali, T.J. Daou, J. Patarin, Phys. Chem. Chem. Phys. 16 (2014) 17893–17899, https://doi.org/10.1039/c4cp01862a.

[34] J.-L. Paillaud, B. Harbuzaru, J. Patarin, Microporous Mesoporous Mater. 105 (2007) 89–100, https://doi.org/10.1016/j.micromeso.2007.03.046.

[35] A. Ryzhikov, I. Khay, H. Nouali, T.J. Daou, J. Patarin, RSC Adv. 4 (2014) 37655–37661, https://doi.org/10.1039/C4RA05519E.

[36] F. Rouquerol, J. Rouquerol, K. Sing, Adsorption by Powders & Porous Solids, Academic Press, 1999.

[37] M. Thommes, K. Kaneko, A.V. Neimark, J.P. Olivier, F. Rodriguez-Reinoso, J. Rouquerol, K.S.W. Sing, Pure Appl. Chem. 87 (2015) 1051–1069, https://doi. org/10.1515/pac-2014-1117.

[38] N. Desbiens, I. Demachy, A.H. Fuchs, H. Kirsch-Rodeschini, M. Soulard, J. Patarin, Angew. Chem. Int. Ed. 44 (2005) 5310–5313, https://doi.org/10.1002/ anie.200501250.

[39] Y.G. Bushuev, G. Sastre, J.V. de Julian-Ortiz, J. Galvez, J. Phys. Chem. C 116 (2012) 24916–24929, https://doi.org/10.1021/jp306188m.

[40] A. Boultif, D. Louer, J. Appl. Crystallogr. 24 (1991) 987–993, https://doi.org/ 10.1107/S0021889891006441.

[41] A. Le Bail, H. Duroy, J.L. Fourquet, Mater. Res. Bull. 23 (1988) 447–452, https:// doi.org/10.1016/0025-5408(88)90019-0.

[42] P. Wagner, S. Zones, M.E. Davis, R.C. Medrud, Angew. Chem. Int. Ed. 38 (1999) 1269–1272, https://doi.org/10.1002/(SICI)1521-3773(19990503)38:9< 1269:: AID-ANIE1269> 3.0.CO, 2-3.

[43] C.A. Fyfe, D.H. Brouwer, A.R. Lewis, L.A. Villaescusa, R.E. Morris, J. Am. Chem. Soc. 124 (2002) 7770–7778, https://doi.org/10.1021/ja012558s.

[44] L.A. Villaescusa, P.A. Barrett, M.A. Camblor, Chem. Commun. 21 (1998) 2329–2330, https://doi.org/10.1039/A806696E.

[45] B.H. Toby, R.B. Von Dreele, J. Appl. Crystallogr. 46 (2013) 544–549, https://doi. org/10.1107/S0021889813003531.